Developmental Biology 431 (2017) 134–144

Contents lists available at ScienceDirect

Developmental Biology

journal homepage: www.elsevier.com/locate/developmentalbiology

Decoupling brain from nerve cord development in the annelid *Capitella teleta*: Insights into the evolution of nervous systems

Allan M. Carrillo-Baltodano, Néva P. Meyer*

Biology Department, Clark University, Worcester, MA 01610, USA

ARTICLE INFO

Keywords:
Neural specification
Spiralian
Annelid
Blastomere isolation
Autonomous

ABSTRACT

In the deuterostomes and ecdysozoans that have been studied (e.g. chordates and insects), neural fate specification relies on signaling from surrounding cells. However, very little is known about mechanisms of neural specification in the third major bilaterian clade, spiralians. Using blastomere isolation in the annelid *Capitella teleta*, a spiralian, we studied to what extent extrinsic versus intrinsic signals are involved in early neural specification of the brain and ventral nerve cord. For the first time in any bilaterian, we found that brain neural ectoderm is autonomously specified. This occurs in the daughters of first-quartet micromeres, which also generate anterior neural ectoderm in other spiralians. In contrast, isolation of the animal cap, including the 2d micromere, which makes the trunk ectoderm and ventral nerve cord, blocked ventral nerve cord formation. When the animal cap was isolated with the 2D macromere, the resulting partial larvae had a ventral nerve cord. These data suggest that extrinsic signals from second-quartet macromeres or their daughters, which form mesoderm and endoderm, are required for nerve cord specification in *C. teleta* and that the 2D macromere or its daughters are sufficient to provide the inductive signal. We propose that autonomous specification of anterior neural ectoderm evolved in spiralians in order to enable them to quickly respond to environmental cues encountered by swimming larvae in the water column. In contrast, a variety of signaling pathways could have been co-opted to conditionally specify the nerve cord. This flexibility of nerve cord development may be linked to the large diversity of trunk nervous systems present in Spiralia.

1. Introduction

Where studied, neural development usually begins with a region of ectoderm receiving extrinsic signals instructing it to become neural (Stern, 2005). Our understanding of this process largely comes from data on two of three major bilaterian clades, deuterostomes (Alvarez et al., 1998; Bertrand et al., 2003; Lea et al., 2009; Muñoz-Sanjuán and Brivanlou, 2002; Pera et al., 2003; Rentzsch et al., 2004) and ecdysozoans (Gómez-Skarmeta et al., 2003; Skeath, 1998; von Ohlen and Doe, 2000). In vertebrates and insects, neural specification is linked to dorsal-ventral (D-V) axis specification and involves multiple signaling events. In vertebrates, neural tissue arises from future dorsal ectoderm and relies in part on inhibition of BMPs by graded antagonists secreted from the organizer (e.g. Chordin, Noggin, and Follistatin) as well as signaling by FGFs and Wnts (De Robertis and Kuroda, 2004; Stern, 2006, 2005; Wilson and Edlund, 2001). In *Drosophila melanogaster*, a ventral-to-dorsal gradient of nuclear Dorsal (NF-κB) protein in the early embryo helps establish the D-V axis, including the region of neurogenic ectoderm. This is achieved by regulating components of other signaling pathways including EGFR and Dpp (BMP2/4). Dorsal upregulation of *rhomboid* generates a gradient of EGFR signaling in the lateral (future ventral) ectoderm, which helps define the neurogenic domain. Dorsal also upregulates *sog* (*chordin*) in the lateral ectoderm, thus generating a dorsal gradient of Dpp (BMP2/4) signaling (Bier, 2011; Ferguson and Anderson, 1992; Irish and Gelbart, 1987; Lynch and Roth, 2011; von Ohlen and Doe, 2000; Wilson et al., 2014).

Very little is known about neural specification in the third major bilaterian clade, spiralians. Classic studies using blastomere isolation in several organisms, including spiralians, have contributed to our understanding of the role of autonomous and conditional fate specification of multiple tissues including neural ectoderm (Fig. 1A and B) (Costello, 1945; Goldstein, 1993; Novikoff, 1938; Reverberi, 1971; Thorpe et al., 1997; Wikramanayake and Klein, 1997). Many taxa within Spiralia have a stereotypical cleavage pattern called spiral cleavage, allowing cell fate and lineage to be compared across taxa (Hejnol, 2010; Lambert, 2010). Starting at the third round of divisions in these animals, the four blastomeres (A–D) cleave asymmetrically to generate a 'first-quartet' of smaller micromeres at the animal pole (1a–1d, also

* Corresponding author.
E-mail address: nmeyer@clarku.edu (N.P. Meyer).

http://dx.doi.org/10.1016/j.ydbio.2017.09.022
Received 21 July 2017; Received in revised form 17 September 2017; Accepted 17 September 2017
Available online 21 September 2017

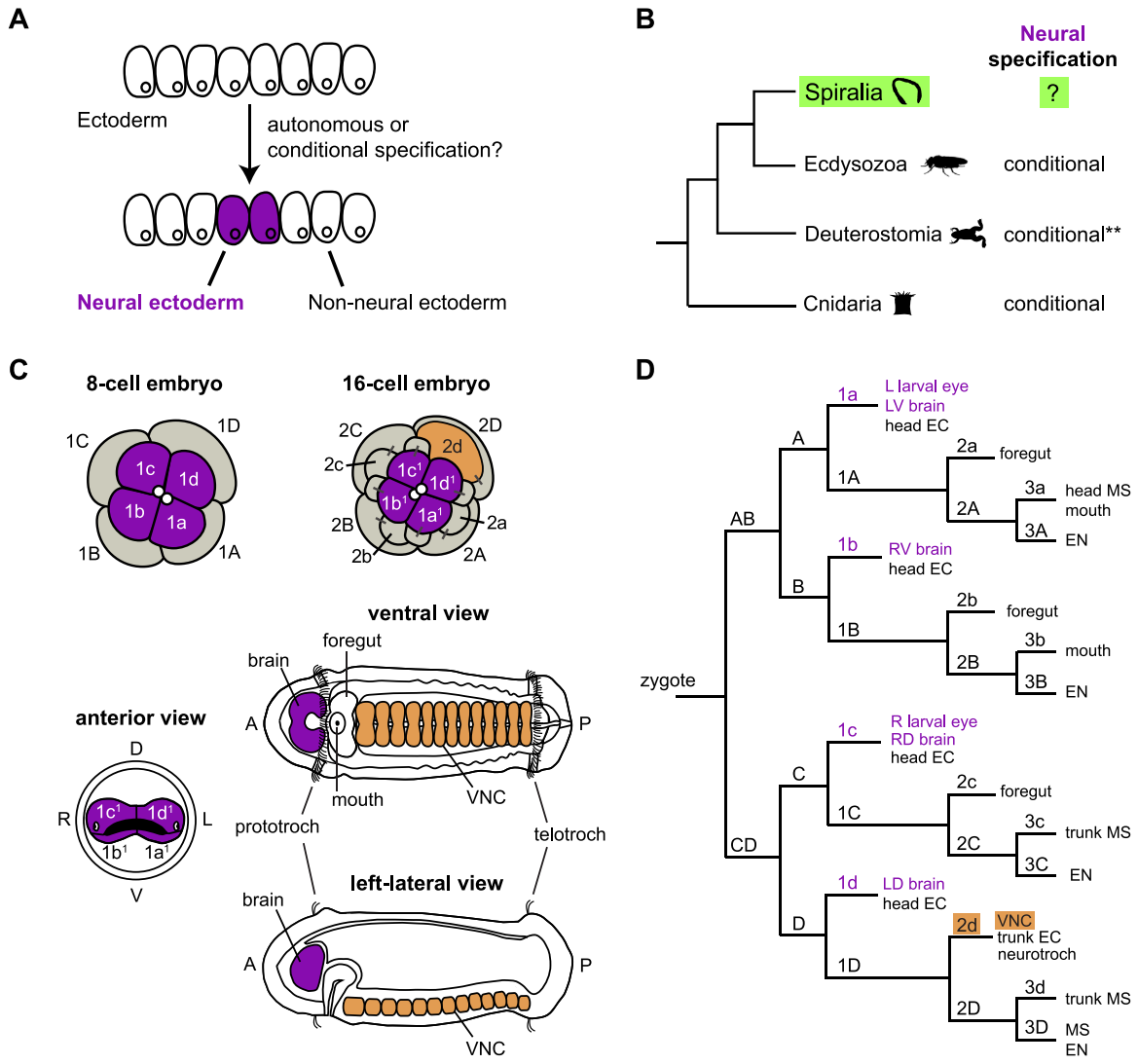

Fig. 1. Early neural ectoderm specification across Bilateria and neural fate map in the annelid *Capitella teleta*. (A) Ectoderm receives early signals instructing formation of neural versus non-neural ectoderm. (B) Generalized phylogeny of Bilateria and its sister group Cnidaria, showing that in the organisms studied so far, neural specification is achieved via extrinsic signals (conditional specification). ** Within Deutorostomia, autonomous specification of the nerve cord has been reported in two species of ascidians (Hudson, 2003; Minokawa et al., 2001). In Spiralia, the mechanisms involved in neural specification are unknown. (C) Diagrams (modified from Meyer et al. (2010)) showing spiral cleavage in 8- and 16-cell embryos and the larval body plan at stage 6 in the annelid *Capitella teleta*. Blastomeres that generate the brain (purple) and ventral nerve cord (orange) are indicated. Blastomere nomenclature is as in Conklin (1897). (D) Lineage diagram (modified from Meyer et al. (2010)) showing the fates of early blastomeres in *C. teleta*. The cells that make the brain (micromeres 1a–1d) are in purple, and the cell that makes the vast majority of the ectoderm in the trunk, including the ventral nerve cord, (micromere 2d) is in orange. A: anterior; D: dorsal; EC: ectoderm; EN: endoderm; L: left; LD: left-dorsal; LV: left-ventral; MS: mesoderm; P: posterior; R: right; RD: right-dorsal; RV: right-ventral; VNC: ventral nerve cord.

referred to as 1q) and larger macromeres at the vegetal pole (1A–1D, also referred to as 1Q) (Conklin, 1897) (Fig. 1C). Daughters of 1q micromeres ($1q^1$) generate anterior neural ectoderm in many spiralians (Ackermann et al., 2005; Dictus and Damen, 1997; Hejnol et al., 2007; Henry et al., 2004; Henry and Martindale, 1998; Huang et al., 2002; Render, 1991; Wilson, 1892). Furthermore, the 1q blastomeres and their descendants asymmetrically inherit maternal mRNAs (Henry et al., 2010; Kingsley et al., 2007; Lambert and Nagy, 2002; Nakamura et al., 2017), although the functions of most of these mRNAs remain unknown and none have yet been identified as neural determinants. One maternal mRNA, *IoLR5*, is necessary for development of the eyes and ciliary bands in the episphere of the snail *Tritia obsoleta* (previously known as *Ilyanassa obsoleta*) (Rabinowitz and Lambert, 2010).

The lineages that contribute to trunk neural ectoderm are more variable in spiralians (Boyer et al., 1998, 1996; Dictus and Damen, 1997; Hejnol et al., 2007; Henry et al., 2004; Henry and Martindale, 1998; Meyer et al., 2010; Render, 1997). In annelids, one cell at the 16-cell stage, the 2d micromere, generates the entire trunk ectoderm and ventral nerve cord (VNC) (Fig. 1C) (Ackermann et al., 2005; Anderson, 1959; Huang et al., 2002; Meyer and Seaver, 2010; Wilson, 1892). In contrast, 2d in mollusks makes only portions of the foot and shell gland (Dictus and Damen, 1997; Hejnol et al., 2007; Render, 1997). Furthermore, the D-quadrant, including 2d, is conditionally specified in some spiralians (Henry and Perry, 2008; Martindale et al., 1985), and subsequently acts as an organizer, specifying the dorsal-ventral (D-V) axis and certain tissues in both the head and the trunk (reviewed in Henry (2014) and Lambert (2008)).

Comparisons of fate maps across annelids and mollusks suggests that there may be differences in neural fate specification between the brain and ganglia in the trunk as these tissues are generated from different lineages. To begin to address this question, we examined neural specification in the annelid *Capitella teleta*, whose brain is derived from daughters of 1q micromeres ($1q^1$) and whose VNC is derived from daughters of 2d ($2d^{1121}$ and $2d^{1122}$; Fig. 1C and D) (Meyer et al., 2010; Meyer and Seaver, 2010). In addition to generating the VNC, the 2d micromere in *C. teleta* has been hypothesized to act as the organizer. However, laser ablation of 2d did not block expression of

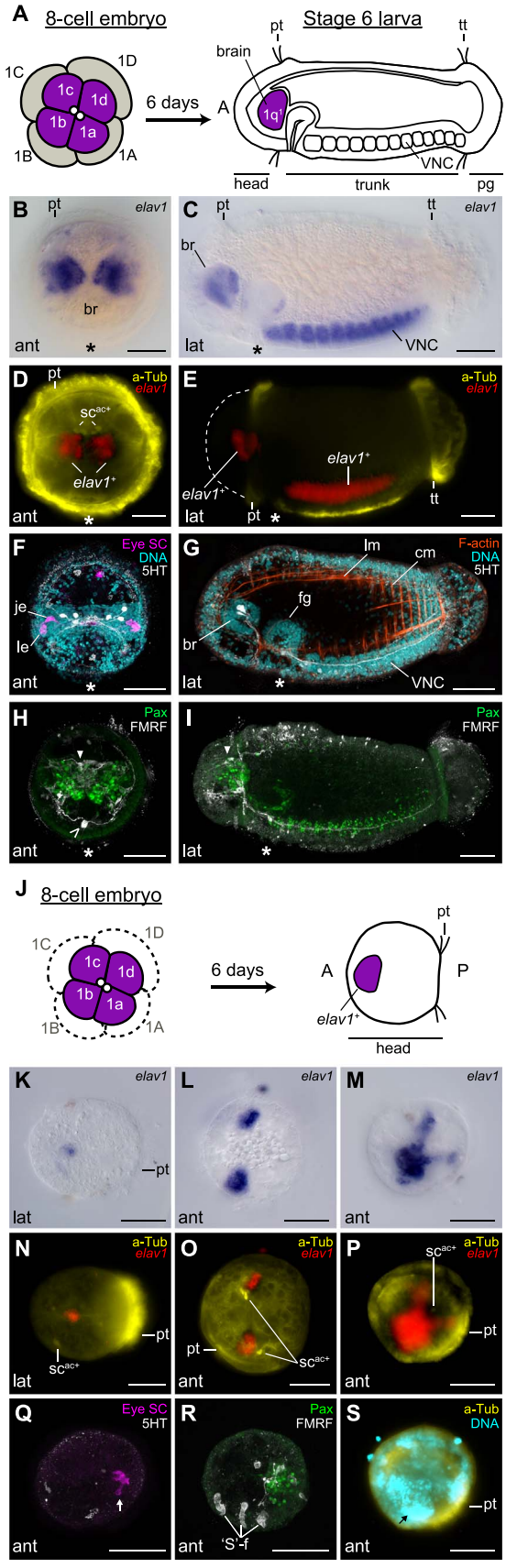

Fig. 2. Partial larvae derived from isolation of first-quartet (1a–1d) micromeres. (A) Diagram of an 8-cell, control embryo showing the first-quartet micromeres, 1a–1d (purple), whose daughters, $1a^1$ – $1d^1$ ($1q^1$ collectively) form the larval brain (purple) after six days. (B–I) Stage 6 larvae derived from a whole-embryo control. B, D, F, and H are images of the two lobes of the brain (br) from an anterior view, ventral down. C, E, G, and I are images of the left-brain lobe (br) and the ventral nerve cord (VNC) from a left-lateral view, anterior left. An asterisk marks the position of the mouth. (J) Diagram of isolated 1a–1d micromeres from an 8-cell embryo, which form a partial larva consisting of a swimming head with neural tissue after six days. (K–S) Partial larvae derived from isolated 1a–1d micromeres, which would normally form the head ectoderm including the brain and prototroch. Lateral views have the prototroch positioned to the right of the panel. Anterior views have the anterior end of the larva towards the reader. Panels B, C, and K–M show expression of *Ct-elav1*, a marker of differentiating neurons. Panels D, E, and N–P are Z-stack projections of widefield images showing false-colored *Ct-elav1* expression (red) and anti-acetylated-Tubulin (yellow, cilia) staining. Panels F–I and Q–S are CLSM z-stacks of different labels as follows. (F, Q) Cyan: TO-PRO-3 (DNA); white: anti-serotonin; magenta: 22C10 (larval and juvenile eye sensory cells). (G) Cyan: TO-PRO-3 (DNA); orange: F-actin (muscle fibers); white: anti-serotonin. (H, I, R) White: anti-FMRF; green: DP311 (Pax). (S) Cyan: Hoechst (DNA); yellow: anti-acetylated-Tubulin (cilia). The same animals are shown in K and N, L and O, and M, P, and S. The closed arrowhead in H and I points to $FMRF^+$ neurons in the brain while the open arrowhead in H points to the anterior mouth cell (F-AMC, (Meyer et al., 2015)) in the trunk. The arrow in Q points to the sensory cell of the larval eye. The arrow in S points to a cluster of nuclei. Number of animals with phenotypes shown above is provided in Table S1. 5HT: serotonin; br: brain; cm: circular muscles; fg: foregut; je: juvenile-eye sensory cell; le: larval-eye sensory cell; lm: longitudinal muscles; pt: prototroch; sc^{ac+}: acetylated-$Tubulin^+$ cells; SC: sensory cell; 'S'-f: 'S'-shaped $FMRF^+$ cell; tt: telotroch; VNC: ventral nerve cord. All scale bars are 50 μm.

the pan-neural gene *Ct-elav1* (Amiel et al., 2013). This result suggests that the brain could be specified autonomously in the $1q^1$ blastomeres and their daughters by asymmetric inheritance of determinants. Alternatively, one or all of the remaining macromeres (2A, 2B, 2C, and 2D) could induce brain fate in the $1q^1$ cells. There is less evidence supporting either autonomous or conditional specification of VNC fate in 2d. Ablation of the C, 2D, 3D, or 2D+3D macromeres in *C. teleta* resulted in larvae with a fairly normal body plan and D-V axis, and animals in which 2D+3D was ablated may have had a VNC based on a nuclear staining and labeling with anti-acetylated-tubulin (Amiel et al., 2013). However, *Ct-elav1* expression was not examined in these animals. Because secreted factors such as Chordin/Sog, FGFs and/or EGFs are important for neural induction in arthropods and deuterostomes, we hypothesized that VNC fate in *C. teleta* is conditionally specified in the 2d cell or its daughters by neighboring cells. Because ablation of 2D+3D may not block VNC formation, it is possible that all second-quartet macromeres produce an inductive signal and that the factors necessary to respond to this signal are asymmetrically segregated to the 2d micromere and subsequently to its daughters to generate the VNC. Alternatively, an inductive signal could be restricted to the D quadrant, specifically 2D or its daughters, and all second-quartet micromeres (2q) could be competent to respond. In this scenario, 2d would be induced to produce neural tissue because of its close proximity to 2D.

2. Results and discussion

2.1. Isolated 1q micromeres form brain tissue

To distinguish between intrinsic and extrinsic signals during neural specification in *C. teleta*, we isolated and cultured blastomeres from 2- to 16-cell embryos using a combination of chemical and mechanical treatments, and compared them with normal larvae developed from whole-embryo controls. After six days, whole-embryo controls developed into normal, segmented metatrochophore larvae divided into a head, trunk, and pygidium (Fig. 2A) (Seaver et al., 2005). In normal larvae, the trunk is delimited by two ciliary bands, the anterior prototroch and the posterior telotroch (Fig. 2A and E). The anterior brain and the VNC in the trunk contain a large number of differentiating neurons, as seen by expression of the pan-neural marker *Ct-elav1* (Fig. 2B–E) (Meyer and Seaver, 2009) and the presence of serotonin$^+$ ($5HT^+$) and $FMRF^+$ neurons and axons (Fig. 2F–I) (Meyer et al., 2015). Pax expression also is visible in the brain and VNC at stage 6 (Fig. 2H and I). In addition to the brain, the anterior neural system (ANS; defined here as all neural cell types derived from 1q (Marlow et al.,

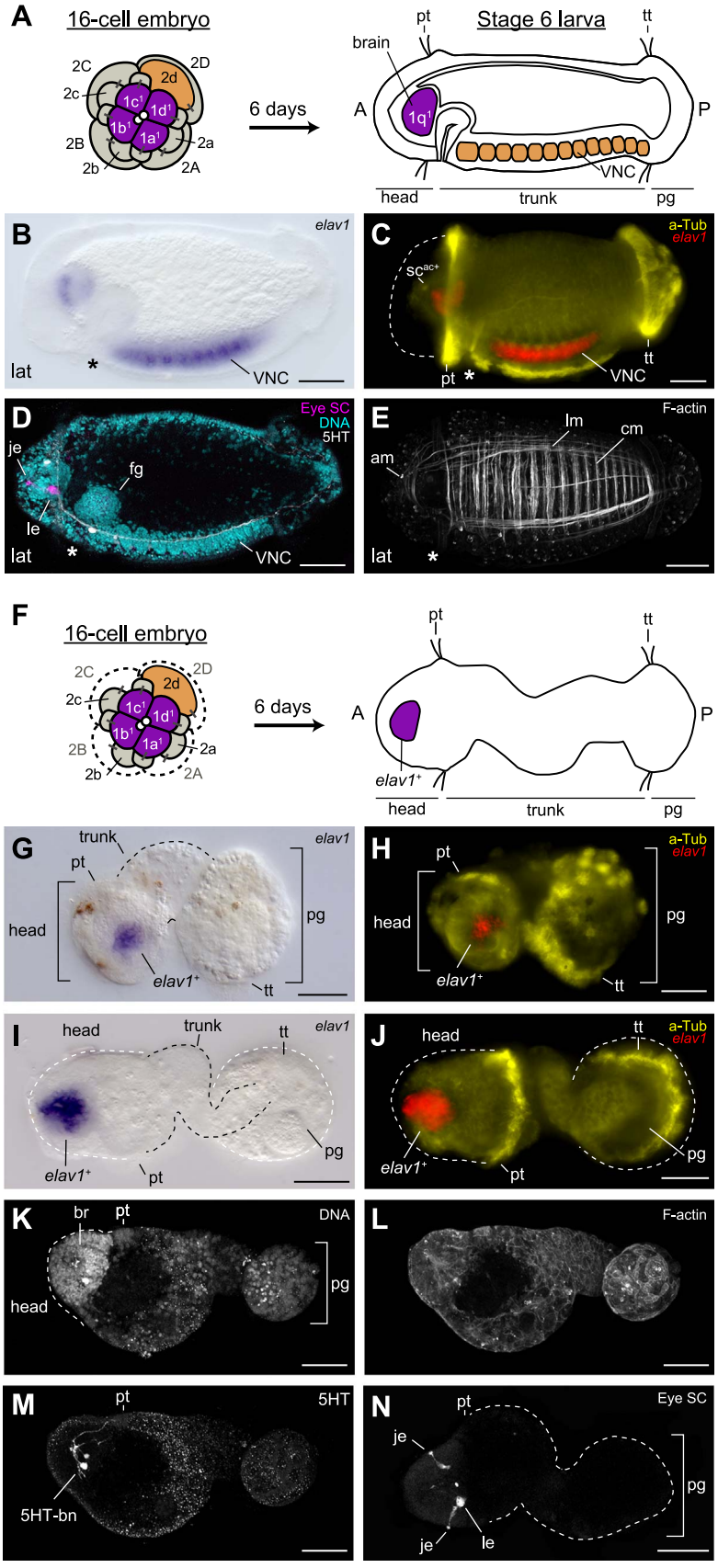

Fig. 3. Partial larvae derived from isolation of animal cap micromeres, including 2d. (A) Diagram of a whole-embryo control showing the fate of first-quartet micromeres $1a^1$–$1d^1$ (purple) and the 2d micromere (orange), which form the larval brain and ventral nerve cord, respectively, after six days. (B–E) Stage 6 larvae derived from a whole-embryo controls. All are images of the left-brain lobe and the ventral nerve cord (VNC) from a left-lateral view, anterior left. An asterisk marks the position of the mouth. (F) Diagram of isolated first- and second-quartet micromeres, including 2d, which form a partial larva with a head with neural tissue and an elongated trunk comprising ectoderm but no neural tissue or muscle fibers after six days. (G–N) Partial larvae derived from isolated first- and second-quartet micromeres, including 2d. Panels B, G, and I show expression of *Ct-elav1*, a marker of

differentiating neurons. Panels C, H, and J are Z-stack projections of widefield images showing false-colored *Ct-elav1* expression (red) and anti-acetylated-Tubulin (yellow) staining. Panels D, E, and K–N are CLSM z-stacks of different labels as follows. (D) Magenta: 22C10 (eye sensory cells); cyan: TO-PRO-3 (DNA); white: anti-serotonin. (E, L) F-actin (muscle fibers). (K) TO-PRO-3 (DNA). (M) anti-serotonin. (N) 22C10 (eye sensory cells). The same animals are shown in G and H, I and J, and K, L, and M. In G, the trunk is demarcated with a dashed line while in G and H, the head and pygidium (pg) are indicated with brackets. In I, the trunk is demarcated with black dashed lines while in I and J, the head and pygidium are marked with white dashed lines. In K, the head is outlined with a dashed line and the pygidium is bracketed. In N, the trunk plus pygidium is outlined with a dashed line and the pygidium is bracketed. Number of animals with phenotypes shown above is provided in Table S1. 5HT: serotonin; 5HT-bn: serotonin^{+} brain neurons; am: anterior muscles; br: brain; cm: circular muscles; fg: foregut; je: juvenile-eye sensory cell; le: larval-eye sensory cell; lm: longitudinal muscles; pg: pygidium; pt: prototroch; sc^{ac+}: acetylated-Tubulin^{+} cells; SC: sensory cell; tt: telotroch; VNC: ventral nerve cord. All scale bars are 50 μm.

2014; Wanninger, 2008; Williams et al., 2017)) also contains two clusters of acetylated-tubulin^{+} sensory cells (sc^{ac+}) positioned dorsal to the brain (Fig. 2D) (Amiel et al., 2013; Meyer et al., 2015) and one pair of differentiated larval eyes and one pair of presumptive juvenile eyes positioned on the left and right sides of the brain (Fig. 2F). Each larval and juvenile eye has one sensory cell, which can be visualized with 22C10 (Yamaguchi and Seaver, 2013) (Fig. 2F le and je, respectively), and the larval eyes also have one orange pigment cell (Rhode, 1993). Other tissues present in stage 6 larvae include longitudinal and circular muscle fibers derived from third- and fourth-quartet micromeres (3a, 3c, 3d, and 4d) and a developing foregut derived from the 2q micromeres (Fig. 2G) (Boyle and Seaver, 2008; Hill and Boyer, 2001; Seaver et al., 2005). Additional FMRF immunoreactivity is present in 'S-shaped' cells throughout the ectoderm while additional DP311 (Pax) immunoreactivity is present in a small subset of cells around the foregut and in the mesoderm, and weakly in cells of the prototroch and telotroch.

To test whether or not the brain is autonomously specified in *C. teleta*, we isolated micromeres 1a–1d (1q). After six days, these partial larvae expressed the pan-neural gene *Ct-elav1* (n=26/26; Fig. 2J–P). The partial larvae appeared to be a swimming 'head' (Fig. 2J; Table S1) with a prototroch at one end, which we inferred to be the posterior end (Fig. 2K–P). We observed *Ct-elav1* expression in one (n=16/26; Fig. 2K and N) or two domains (n=7/26; Fig. 2L and O), sometimes with extended posterior projections (n=3/26; Fig. 2M and P). Clusters of sc^{ac+} cells were present near the *Ct-elav1* expressing domains, but in a varied number and position (Fig. 2N–P). This supports the interpretation that *Ct-elav1* was expressed in brain tissue in the 1q-derived partial larvae because these cells are normally associated with the brain. However, the disorganization of the sc^{ac+} clusters and the presence of one or two *Ct-elav1*$^{+}$ domains with occasional posterior projections suggests a lack of bilateral and possibly D-V symmetry in the swimming heads. In further support of the head identity of the partial larvae, some had the orange pigment cells of the larval eyes (Video 1; Table S1) and the sensory cells of the larval and juvenile eyes (Fig. 2Q; Table S1), which are also normally associated with the brain. We also found Pax^{+} cells (n=17/17) and one or two FMRF^{+} neurons (n=14/17), further confirming the formation of neural tissue in the 1q-derived partial larvae. Finally, we saw several 'S'-shaped FMRF^{+} cells ('S'-f) (n=13/17) (Fig. 2R) and clusters of more densely packed nuclei (e.g. black arrow in Fig. 2S) that were associated with *Ct-elav1* expression where examined and likely represented brain tissue. Interestingly, we did not detect serotonin^{+} neurons (n=0/33) in the 1q-derived partial larvae (Fig. 2Q, R), indicating that these cells may either be specified conditionally or that they may derive from a lineage other than 1q (discussed further below). Finally, the segregation of the different neural and ciliary markers demonstrates that these partial larvae formed and partitioned neural, non-neural, and prototrochal fates.

Given that our isolation approach removed all other blastomeres, it provides new insight into the autonomous specification of anterior neural tissue in the 1q cells. Similar to our findings, laser ablation experiments in *C. teleta* have shown that the D cell at the 4-cell stage, 1D at 8-cell stage, or 2d and 2D at the 16-cell stage are not necessary for anterior neural specification (Amiel et al., 2013). Taken together, both blastomere isolation (this study) and laser ablation (Amiel et al., 2013) experiments demonstrate that 1q micromeres in *C. teleta* may form brain tissue by inheriting maternal determinants at the third division, and do not require extrinsic signals from the 1Q macromeres, or subsequent lineages including the hypothesized organizer 2d, mesoderm, or endoderm. Alternatively, cells other than the brain precursors could inherit determinants, and later conditional signaling between the daughters of 1q could then specify neural fate. Previous fate-mapping experiments in *C. teleta* found that the 1q^{1} blastomeres contribute to neural and non-neural ectoderm while the 1q^{2} blastomeres form the prototroch (Fig. 1D) (Meyer et al., 2010). Additional lineage tracing done by Eisig in 1898 found that the 1q^{111} blastomeres form both neural and non-neural ectoderm in *Capitella capitata* (Eisig, 1898). This suggests that although neural (or other) determinants may be inherited by the 1q blastomeres at the 8-cell stage, neural specification occurs much later in a subset of their descendants.

2.2. Isolated 1q and 2q micromeres do not form the ventral nerve cord

In order to test if specification of the VNC in the trunk requires extrinsic signals, we tried to isolate 2d at 13- to 16-cell stages. However, isolated 2d blastomeres lysed within hours or days. Costello (1945) was capable of isolating 2d blastomeres from only three embryos of the annelid *Alitta succinea* (previously *Nereis limbata*), but also found that they arrested after cleaving several times. To overcome this, we isolated the animal cap as soon as 2d was born. This included 2d plus the other 1q and 2q micromeres. This allowed us to test if the second-quartet macromeres (2Q; i.e. vegetal pole), which form endoderm and mesoderm, send extrinsic signals to 2d or its daughters to induce neural tissue of the VNC. The whole-embryo controls had a brain and VNC that expressed *Ct-elav1*, in addition to mesodermal and endodermal tissues (Fig. 3A–E). Also visible were the prototroch and telotroch, as well as the neurotroch, which is positioned at the ventral midline below the VNC (Fig. 3C).

When we isolated animal caps at the 16-cell stage, about half of them (n=25/52) developed into elongated, swimming larvae with a head, a trunk delimited by a prototroch and telotroch, and a pygidium (Fig. 3F–N; Table S1), as expected from the fate map (Meyer et al., 2010). The other half developed into swimming larvae with a head and a shortened trunk (n=27/52; Table S1), which we think resulted from improper division of 2d. In the animals with an elongated trunk, we did not detect ganglia, serotonergic neurons, or expression of *Ct-elav1* (n=0/18) between the prototroch and telotroch (Fig. 3G–J), indicating that these larvae lacked a VNC. In contrast, the tissue anterior to the prototroch expressed *Ct-elav1* (n=13/18), coincident with a high density of nuclei, which we interpret as the brain (Fig. 3G–K; Table S1). As further confirmation that *Ct-elav1* expression was in brain tissue in larvae derived from animal caps isolated at the 16-cell stage, we detected the pigment and sensory cells of larval eyes, the sensory cells of the juvenile eyes (Fig. 3N; Video 2; Table S1), and the sc^{ac+} cells (Table S1) on one end of the partial larvae. Unexpectedly, we also detected serotonin^{+} neurons in the head (n=24/24), which sent axons posteriorly towards the elongated trunk (Fig. 3M). The head of the animal cap isolates appeared to have bilateral symmetry and a D-V axis, as seen by the formation of two brain lobes and lack of *Ct-elav1*$^{+}$ posterior projections. Both of these findings are in contrast to the 1q isolates, which lacked serotonin^{+} neurons and did not have clear D-V or left-right axes. Within the trunk, the neurotroch ciliary band serves both as a marker of cell fate, since it is mostly derived from daughters of 2d (Fig. 1D) (Meyer and Seaver, 2010), and a D-V marker, since it is

localized to the ventral midline (Fig. 3C). Within the trunks of the animal-cap larvae, we detected scattered cells with tufts of cilia that could be remnants of the neurotroch (Table S1), but these cells were not localized to one side of the animal, suggesting a loss of the D-V axis in the trunk. Based on nuclear staining and DIC microscopy, the animal-cap larvae lacked a foregut (data not shown), which is normally derived from the 2a–2c micromeres (Fig. 1D) (Meyer et al., 2010). However, this should be confirmed with additional molecular markers in the future. We also did not detect any yolk granules based on DIC microscopy or muscle fibers based on staining for f-actin, confirming the absence of endodermal and mesodermal fates, respectively (Fig. 3G, I, and L). As mesoderm and endoderm is normally generated by daughters of second-quartet macromeres (Meyer et al., 2010), this further verifies their removal in the animal-cap isolates.

Blastomere isolation and ablation experiments have shown that the D quadrant can develop into an almost normal larva in some spiralians (Clement, 1956; Wilson, 1904a, 1904b), making it plausible that the 2D macromere or its descendants are sufficient to induce trunk neural fate. In order to test this possibility, we isolated the animal cap (including 2d) plus the 2D macromere at the 16-cell stage (SFig. 1, Table S1). We found that 13 out of 16 animals had ganglia in the trunk, and 12 of these expressed *Ct-elav1* in the ganglia, demonstrating that 2D or its descendants are sufficient to induce formation of the VNC. In these isolations, we also observed the presence of a foregut (n=12/16; SFig. 1D, H), a neurotroch that was localized to the ventral side of the larvae (n=15/16; SFig. 1C, E, F, I), and yolky endoderm (e.g. SFig. 1F).

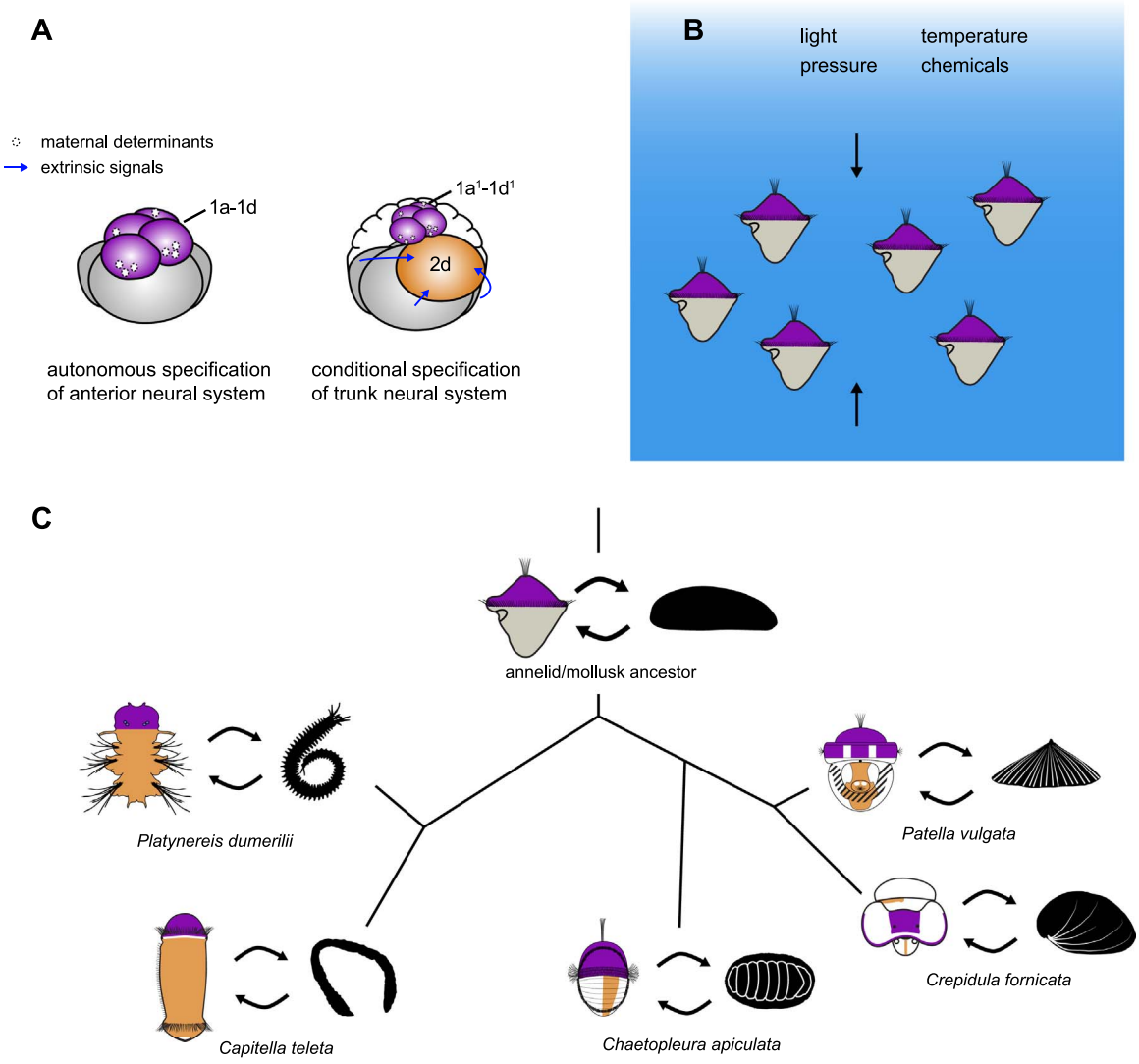

Fig. 4. Models of evolution of the head and trunk in spiralians. (A) The anterior neural system (ANS), including the brain, of spiralians is autonomously specified by asymmetric inheritance of maternal determinants into the first-quartet micromeres, 1a–1d (purple). In contrast, the trunk neural system (ventral nerve cord in annelids) is conditionally specified in the appropriate micromere(s) (2d micromere in annelids, orange) by extrinsic signals from neighboring blastomeres. The BMP, MAPK and/or Wnt signaling pathways are potential candidates for this neural inducing signal. Modified from Henry (2014) with permission from UPV/EHU Press. (B) The last common ancestor of annelids and mollusks, and possibly all spiralians, had a swimming larval stage in which early ANS formation in the head (purple) was selected for, enabling the larva to respond to environmental cues in the water column. A rapid and restricted specification of the ANS, such as by inheriting maternal mRNAs and proteins, may have enhanced success and survival of the swimming larva. Adapted from Nielsen (2012) with permission of CSIRO Publishing and (Conzelmann et al., 2011) with permission from PNAS. (C) In the ancestor of annelids and mollusks, and possibly all spiralians, the first-quartet micromeres, 1a–1d, developed an ANS via autonomously specification. This is supported by the conserved fate of 1a–1d, which form the head, including the brain and the prototroch (purple). In contrast, the blastomeres that formed the trunk and nerve cord diverged in different lineages. For example, in annelids (e.g., *Platynereis dumerilii* and *Capitella teleta*) the 2d micromere makes the entire post-trochal ectoderm (orange) including all of the ventral nerve cord; whereas, in mollusks (e.g., *Patella vulgata*, *Crepidula fornicata*, and *Chaetopleura apiculata*), the 2d micromere only generates a portion of the foot and shell gland (orange) (Dictus and Damen, 1997). The ability of different signaling pathways to specify neural tissue at later time points in the trunk may have provided flexibility, possibly resulting in morphological divergence in spiralian nerve cords. Diagrams adapted from Dickinson et al. (1999), Dictus and Damen (1997), Henry et al. (2004) and Williams et al. (2014), with permission from ElSevier and Springer Nature. Silhouettes of *P. dumerilii* and *C. teleta* available in PhyloPic (www.phylopic.org), by Duygu Özpolat and Frank Föster, respectively.

The left mesodermal band also was presumably present, but muscle fibers were not examined.

As further evidence that the D quadrant is sufficient to specify VNC tissue in *C. teleta*, we isolated the D macromere at the 4-cell stage (SFig. 2, Table S1), which should generate brain tissue (1d), trunk ectoderm including the VNC and neurotroch (2d), and mesoderm and endoderm (2D). Partial larvae derived from the D macromere had *Ct-elav1* expression in the head (n=14/17) and trunk (n=5/17; SFig. 2G, H) and serotonin$^+$ neurons and axons in the head and trunk (n=7/7; SFig. 2C, E, arrows), indicating that these animals formed a brain and VNC. We also detected ectopic *Ct-elav1* expression in the pygidium in one animal (n=1/17; SFig. 2G, H). Some of the animals had cilia in the trunk, likely the neurotroch, but the cilia were not localized to one side of the animal (n=3/7). Finally, these larvae had muscle fibers (n=7/7; SFig. 2C, F) and yolky endoderm cells (SFig. 2B). These data suggest that 2d in the presence of the 2D macromere is capable of making VNC tissue.

The absence of a VNC in the trunk of larvae derived from isolated animal caps supports the hypothesis that neural tissue in the trunk is conditionally specified in *C. teleta*. Although the molecular pathways responsible for neural specification in the trunk have not yet been identified in annelids (Amiel et al., 2013; Demilly et al., 2013; Denes et al., 2007; Kuo and Weisblat, 2011), we can hypothesize which blastomeres provide the extrinsic signal(s). 1q and 2q micromeres are not sufficient (this study) and 1q is not necessary (Yamaguchi et al., 2016) for VNC specification. 1q also appears to not be necessary for trunk development in the snail *T. obsoleta*, although neural fate was not assessed (Sweet, 1998). We found that 2D is sufficient for VNC specification in *C. teleta* (SFig. 1 and 2). As 2D generates both mesoderm and endoderm, it will be interesting to see if other macromeres such as 2B, which only generates endoderm, are also sufficient to induce neural fate in the trunk of *C. teleta*. Interestingly, the animal cap + 2D isolates appeared to generate more *Ct-elav1*$^+$ ganglia than the D isolates (~8 versus 3 ganglia, respectively; compare SFigs. 1B and 2G); however, there also appeared to be posteriorly-localized ganglia in the D isolates that lacked *Ct-elav1* expression (compare SFig. 2C and G). There are multiple possible explanations for the difference in *Ct-elav1* expression in the trunks of the two sets of isolates. One possibility is that neural differentiation in the D isolates could be delayed since the VNC in *C. teleta* develops from anterior to posterior (Meyer et al., 2015). Another possibility is that micromeres other than 1d and 2d augment fate specification of the VNC, or that multiple inductive events are important for VNC specification.

The 2d micromere itself could be involved in setting up later inductive events (e.g. from the mesoderm), as it is hypothesized to act as the organizer in *C. teleta*. Amiel et al. (2013) ablated 2d in *C. teleta* but the resulting animals still had muscle fibers and yolky endoderm cells and expressed the mesodermal markers *Ct-gataB3* and *Ct-twist1*. Because the mesoderm tissue was greatly reduced in these animals, 2d is important for some mesoderm formation. However, these data make it less likely that 2d specifies mesoderm fate in neighboring cells, which then signal back to 2d to specify neural fate. In contrast, in leech removal of the M teloblast on one side of the animal (resulting in no mesoderm on that side of the animal) or all mesoderm in the mid-body did not block neural specification in the trunk (Torrence et al., 1989). This suggests that neural specification in leech does not rely on an inductive signal from the mesoderm. Furthermore, in leech the neural precursor cells that generate the VNC arise from multiple cell lineages (N, O, P, Q, and M teloblasts) that occupy spatially distinct positions along the D-V axis (Shankland, 1995). Taken together, these data suggest that the mechanism of VNC specification may differ between *C. teleta* and leech.

2.3. Function of the organizer in C. teleta

Organizing activity from the D quadrant has been demonstrated in a number of mollusks and in a few annelids (Amiel et al., 2013; Henry and Perry, 2008; Henry, 2014; Henry et al., 2006; Lambert, 2008; Lambert and Nagy, 2001; Nakamoto et al., 2010). In *C. teleta*, we revealed that the hypothesized organizer in *C. teleta*, 2d (Amiel et al., 2013), is not necessary for specification of the brain, although it may be necessary for specification of serotonin$^+$ neurons in the brain. Larval eyes in *C. teleta* (this study) and in *A. succinea* (Costello, 1945), which are derived from the 1a^1 and 1c^1 micromeres, also can be specified without extrinsic signals from 2d. Interestingly, in the snail *T. obsoleta*, both maternal determinants and an organizing signal from the D-quadrant are necessary for normal eye formation (Clement, 1962; Rabinowitz and Lambert, 2010; Sweet, 1998). The swimming heads derived from 1q in *C. teleta* have an anterior-posterior axis, but we could not identify a clearly defined D-V axis or serotonin$^+$ neurons with our current markers, suggesting that 2d organizing activity may be important for D-V axis specification and formation of serotonin$^+$ neurons in the brain but not anterior-posterior axis formation.

Larvae derived from animal caps isolated at the 16-cell stage had all three axes as well as serotonin$^+$ neurons in the head. This supports the idea that 2d organizes the D-V and left-right axes in the head and either conditionally specifies serotonin$^+$ neurons in the head, or directly generates them since 2d makes a small number of brain cells (Meyer et al., 2010; Meyer and Seaver, 2010). We did not detect a clear D-V axis in the trunk of the animal cap isolates since they lacked a VNC and foregut, and the ciliated cells in the trunk (possibly neurotroch) were disorganized and not concentrated on one side of the larvae. This is in contrast to the animal cap + 2D isolates, in which the foregut, VNC, and neurotroch were all clearly localized to the ventral side of the trunk. This could indicate that cells other than 2d (e.g. 2D or its daughters) organize the D-V axis in the trunk and provide inductive signals for the foregut and VNC, although additional molecular markers should be used to further characterize the phenotypes in the animal cap isolates. Interestingly, Amiel et al. (2013) found that the D macromere but not 2d is necessary for expression of the foregut marker *Ct-foxA*, suggesting that either 2D or its descendants induce foregut tissue in *C. teleta*.

2.4. Implications for evolution of the spiralian head and anterior neural system

Trochophore and metatrochophore larvae of mollusks and annelids share many morphological and molecular similarities across a variety of species (Jägersten, 1972; Marlow et al., 2014; Nielsen, 2005, 2004; Xu et al., 2016), including the anterior pre-trochal region of the larvae (episphere in *bona fide* trochophore larvae). This region is derived from 1q micromeres and is homologous between annelids and mollusks. Furthermore, 1q^1 blastomeres form the brain while 1q^2 blastomeres form primary prototroch cells where examined (Ackermann et al., 2005; Anderson, 1959; Costello, 1945; Dictus and Damen, 1997; Hejnol et al., 2007; Henry et al., 2007, 2004; Henry and Martindale, 1998; Huang et al., 2002; Marlow et al., 2014; Mead, 1897; Meyer et al., 2010; Render, 1991; Wanninger, 2008; Weisblat et al., 1984; Williams et al., 2017; Wilson, 1904a, 1904b, 1892). Based on a few studies, the prototroch and some fates within the larval anterior neural system (ANS) have been shown to be autonomously specified in daughters of 1q. Wilson (1904b) described the formation of the apical organ (part of the ANS in trochophore larvae) from single cell isolations of 1a, 1b, 1c, and 1d in the gastropod *Patella caerulea*, while in the scaphopod *Dentalium* sp., only 1d isolates formed the apical organ (Wilson, 1904a). Likewise, in the annelids *A. succinea* (Costello, 1945) and *Chaetopterus* sp. (Henry, 1986), 1q isolates formed an apical tuft, which is usually associated with the apical organ. Likewise, the prototroch was shown to be autonomously specified in daughters of 1q in *A. succinea*, *Dentalium* sp., and *Patella caerulea* (Costello, 1945; Wilson, 1904a, 1904b). Finally, our results suggest that the ANS, including the brain, and prototroch of *C. teleta* also are autonomously specified.

Based on homology of the 1q lineages in spiralians and the autonomous specification of some 1q fates in a few annelids and mollusks, we hypothesize that ANS and other fates derived from 1q may have been autonomously specified in the last common ancestor of annelids and mollusks (Fig. 4). It has been suggested that autonomous specification evolved to enable the early formation of functional cells (e.g. neurons). Furthermore, autonomously-specified cells/tissues have been suggested to display less plasticity and regulative capacity than conditionally-specified cells/tissues (Davidson, 1990). That is, the presence of determinants may constrain the range of potential fates that a cell can generate. If Davidson's hypothesis is correct, asymmetric inheritance of determinants in the 1q micromeres (Fig. 4A) in the last common ancestor of annelids and mollusks may have resulted in rapid specification and differentiation of the ANS and prototroch. This would have enabled the swimming larvae to sense and respond to environmental cues such as light (Jékely et al., 2008; Randel et al., 2014; Tosches et al., 2014; Zantke et al., 2013), pressure, temperature, and water-borne chemicals (Fig. 4B). Comparing autonomous versus conditional mechanisms of neural specification across Spiralia should help elucidate the relative advantages of these two modes of specification.

2.5. Implications for nerve cord development and evolution of body plans

In contrast to autonomous specification, conditional specification has been suggested to take longer and to have a prolonged period of commitment, during which time cells are able to modify fates based on signals from surrounding tissues (Davidson, 1990). Deuterostomes and ecdysozoans largely undergo conditional neural specification via different combinations of signals including BMPs, Wnts, FGFs, EGFs, and the MAPK cascade (Alvarez et al., 1998; Bertrand et al., 2003; Gómez-Skarmeta et al., 2003; Lea et al., 2009; Muñoz-Sanjuán and Brivanlou, 2002; Pera et al., 2003; Rentzsch et al., 2004; Skeath, 1998; Stern, 2006, 2005; von Ohlen and Doe, 2000). Our study in *C. teleta* shows that specification of the VNC also requires extrinsic signals from the 2Q macromeres (vegetal pole) or their descendants. We think it plausible that conditional neural specification could be more labile than autonomous specification. This plasticity could allow different signaling pathways to drive neural specification and could result in more varied phenotypes, such as the striking morphological diversity of nerve cords seen across Spiralia and Bilateria (Hejnol and Lowe, 2015; Lowe et al., 2006). Remarkably, in two species of ascidians, neural specification of the nerve cord occurs autonomously (Hudson, 2003; Minokawa et al., 2001), while the brain is conditionally specified (Bertrand et al., 2003). Because a large percentage of the ascidian embryo is autonomously specified (Davidson, 1990; Kumano and Nishida, 2007), autonomous neural specification in this species could be linked to factors other than those discussed here.

It has been hypothesized that a BMP-Chordin network was used to induce neural tissue as part of D-V axis specification in the last common ancestor of Bilateria (De Robertis, 2008). In other annelids (*Helobdella* and *P. dumerilli*), BMP signaling does not seem to be important for neural induction, but may be involved in D-V axis specification (Denes et al., 2007; Kuo and Weisblat, 2011). In mollusks, BMPs are important for specification of the shell while their ancestral function during D-V axis and neural specification is not as clear (Hashimoto et al., 2012; Herpin et al., 2007; Iijima et al., 2008; Kin et al., 2009; Lambert et al., 2016; Nederbragt et al., 2002; Tan et al., 2017). In contrast, the MAPK cascade has been shown to function in D-V specification in multiple molluscan species (Henry, 2014; Kozin et al., 2013). Interestingly, a recent study in the snail *T. obsoleta* found that BMP signaling affects D-V specification and may promote rather than inhibit neural formation (Lambert et al., 2016). Given these differences, it is difficult to speculate what the neural inducing signal in annelids is, and it may be a combination of BMP, Wnt, and/or the MAPK cascade (Fig. 4A). In chordates, the importance of BMP antagonism in inducing neural tissue varies depending on organism, and in mice and chick, FGF (via the MAPK cascade) and Wnt signaling play a key role (De Robertis and Kuroda, 2004; Stern, 2006, 2005; Wilson and Edlund, 2001). This has led to the suggestion that neural induction in chordates, which is very likely a homologous process, has undergone developmental system drift (DSD), i.e. the underlying gene regulatory network (GRN) has diverged (True and Haag, 2001). There is also evidence of DSD underlying neural development in insects (Biffar and Stollewerk, 2015, 2014; Suryamohan et al., 2016). Alternatively, in a scenario where BMP/MAPK/Wnt were all used ancestrally to specify neural ectoderm (Arendt and Nübler-Jung, 1997; De Robertis and Sasai, 1996), one or more of these pathways could have lost its function as a neural inducer in different bilaterian lineages, while the remaining pathways could have become sufficient for this specification. It will be interesting to compare mechanisms of trunk neural specification in annelids and mollusks, and, if trunk neural tissue is homologous between these clades (see Hejnol and Lowe (2015)), to gauge if DSD has occurred (Fig. 4C).

3. Conclusions

Our data provided here in the annelid *C. teleta* demonstrate that the brain is autonomously specified in 1q micromeres, while the VNC, derived from 2d, requires extrinsic signals from the 2Q macromeres or their descendants. We also show that the 2D macromere is sufficient to induce neural fate in the VNC. These findings increase our understanding of how neural fate specification is accomplished outside of Ecdysozoa and Deuterostomia and suggest an unusual combination of inherited maternal determinants and signaling pathways that specify neural tissue in the head versus the trunk. Future efforts using a combination of blastomere manipulations and transcriptomic profiling should begin to unravel the gene regulatory networks underlying ANS and trunk neural specification in *C. teleta*. Finally, it will be very exciting to determine if the differences in conditional specification of the trunk neural system are linked with the large diversification of trunk body plans within Spiralia.

4. Materials and methods

4.1. Animal care and embryo collection

Adults of *Capitella teleta* Blake et al. (2009) were cultured in glass finger bowls with artificial sea water (ASW) and fed with sieved mud as in Grassle and Grassle (1976) and Seaver et al. (2005). Females with broods were collected from the lab colony or from mating dishes. For mating dishes, males and females were kept in isolation in separate bowls with mud and ASW for a few days before being combined in the same bowl 12–16 h before collection of the embryos. Embryos were obtained by dissecting the broods with Dumont #5 forceps and transferred with a mouth pipet to 0.22 μm filtered ASW with 60 μg/mL penicillin and 50 μg/mL streptomycin (ASW+PS).

4.2. Blastomere manipulation

Embryos at the selected cleavage stage were incubated in 4-well gelatin-coated dishes with 1x Calcium and Magnesium Free Artificial Sea Water (CMF-ASW) (Strathmann, 1987) for 5–10 min (min), followed by incubation in 1% protease (Sigma-Aldrich cat# P6911) and 1% sodium thioglycolate (Sigma-Aldrich cat# T0632) in CMF-ASW for 5 min rocking at room temperature (~22 °C). Embryos then were washed three times with ASW+PS. After partial dissociation, the selected blastomeres were removed from the rest of the embryo using an eyelash brush and raised individually in ASW+PS for six days in 24-well dishes at 19 °C. The ASW+PS was changed daily. Control embryos from the same brood were kept in ASW+PS in 4-well dishes, with daily ASW+PS water changes.

4.3. Immunohistochemistry

Immunohistochemistry was carried out as in Meyer et al. (2015). Briefly, animals were relaxed with a 1:1 mixture of ASW plus 0.37 M $MgCl_2$ for 12 min before fixing with 4% paraformaldehyde (stock 32% paraformaldehyde from Electron Microscopy Sciences) in ASW for 30 min at room temperature. Fixative was removed by washing several times with 1x PBS and then 1x PBS + 0.1% Triton-X 100 (PBT). Animals were then transferred to RainX-coated three- or nine-well spot glass dishes containing PBT, blocked in 10% goat serum with 1x PBT (block) for 1 h at room temperature, and then incubated in primary antibody in block overnight at 4 °C. After primary incubation, animals were washed several times in PBT and then incubated in secondary antibody overnight at 4 °C. After secondary antibody incubation, animals were washed at room temperature several times over an hour in PBT and quickly washed with PBS to remove the detergent. After the PBS washes, animals were stained for DNA and, if applicable, f-actin in PBS and then cleared and mounted (see Imaging section below). Primary antibodies used were as follows: 1:600 rabbit anti-serotonin (5HT; Sigma-Aldrich, cat #S5545), 1:20 mouse anti-Futsch clone 22C10 (Developmental Studies Hybridoma Bank), 1:800 mouse anti-acetylated tubulin (clone 6-11B-1, Sigma, cat #T6793), 1:10 anti-Pax3/7 (clone DP311 (Davis et al., 2005)). The 22C10 monoclonal antibody developed by S. Benzer and N. Colley was obtained from the Developmental Studies Hybridoma Bank, created by the NICHD of the NIH and maintained at The University of Iowa, Department of Biology, Iowa City, IA 52242. Secondary antibodies used were as follows: 1:300 goat anti-mouse $F(ab')_2$ FITC (Sigma-Aldrich, cat #F8521) and 1:600 sheep anti-rabbit $F(ab')_2$ Cy3 (Sigma-Aldrich, cat #C2306) in block. F-actin and DNA staining were performed by incubating the embryos in 1:100 BODIPY FL-Phallacidin (Life Technologies, cat #B607; stock concentration 200 Units/mL in methanol) and 0.1 µg/mL 33342 Hoechst (Sigma-Aldrich, cat #B2261) or 1:1000 TO-PRO-3 (Life Technologies, cat #T3605) in PBS according to (Meyer et al., 2015, 2010).

4.4. Whole Mount In Situ Hybridization (WMISH)

Animals were relaxed as above and fixed with 4% paraformaldehyde overnight at 4 °C. After fixation, animals were rinsed three times with PBS, and then dehydrated in a series of methanol dilutions (25%, 50%, 75% and 100%) and stored at −20 °C. WMISH was carry out as in Meyer et al. (2015) with a slight modification. Proteinase-K (Invitrogen, cat #59895) was not used in the larvae developed from isolated blastomeres as the egg envelope had already been removed. Animals were hybridized for 72 h at 65 °C with 1 ng/µL of DIG-labeled anti-sense *Ct-elav1* RNA probe as used in Meyer and Seaver (2009). *Ct-elav1* mRNA was detected using a dilution of 1:5000 anti-DIG-AP (Roche) overnight. NBT/BCIP substrate was added to develop a color reaction for 8–43 h at room temperature. The color reaction was stopped using PBS + 0.1% Tween-20 (PTw). Animals were then transferred to 3-well glass dishes, washed several times with PBS and incubated with anti-acetylated tubulin and anti-serotonin following the immunohistochemistry protocol above, and stained with Hoechst. Anti-serotonin was not detected either in isolated embryos or controls after the WMISH.

4.5. Imaging and image handling

WMISH animals were mounted in 80% glycerol in PBS, mounted on glass slides with #1½ coverslips and imaged using DIC optics on an AxioImager M2 compound microscope (Zeiss) coupled with an 18.0 megapixel EOS Rebel T2i digital camera (Canon). Animals for immunofluorescence were mounted and imaged as above, except that an AxioCam MRm rev.3 camera (Zeiss) and Zen Blue software (Zeiss) were used to capture the images. Animals for confocal laser scanning microscopy (CLSM) were cleared and mounted in SlowFade® Gold (Life Technologies, cat# S36936) and imaged using a TCS SP5-X (Leica). For videos 1 and 2, animals were mounted in ASW+PS and recorded with the EOS Rebel T2i as above. DIC images (.TIFF) were rendered in Helicon Focus (HelSoft). Z-projections were obtained from the CLSM scans using Fiji (Image J2, NIH). Contrast and brightness of immunohistochemistry and WMISH images were edited in Photoshop CC, and figure panels were constructed using Illustrator CC (Adobe Systems, Inc.).

Funding

This research did not receive any specific grant from funding agencies in the public, commercial, or not-for-profit sectors.

Conflicts of interest

None.

Acknowledgements

The authors thank R. Bellin at the College of the Holy Cross for access to the confocal microscope and D. Larochelle at Clark University and C. Magie at Quinnipiac University for providing comments on this manuscript.

Appendix A. Supplementary material

Supplementary data associated with this article can be found in the online version at http://dx.doi.org/10.1016/j.ydbio.2017.09.022.

References

Ackermann, C., Dorresteijn, A., Fischer, A., 2005. Clonal domains in postlarval *Platynereis dumerilii* (Annelida: polychaeta). J. Morphol. 266, 258–280. http://dx.doi.org/10.1002/jmor.10375.

Alvarez, I.S., Araujo, M., Nieto, M.A., 1998. Neural induction in whole chick embryo cultures by FGF. Dev. Biol. 199, 42–54. http://dx.doi.org/10.1006/dbio.1998.8903.

Amiel, A.R., Henry, J.Q., Seaver, E.C., 2013. An organizing activity is required for head patterning and cell fate specification in the polychaete annelid *Capitella teleta*: new insights into cell-cell signaling in Lophotrochozoa. Dev. Biol. 379, 107–122. http://dx.doi.org/10.1016/j.ydbio.2013.04.011.

Anderson, D.T., 1959. The embryology of the polychaete *Scoloplos armiger*. Q. J. Microsc. Sci. 100, 89–166.

Arendt, D., Nübler-Jung, K., 1997. Dorsal or ventral: similarities in fate maps and gastrulation patterns in annelids, arthropods and chordates. Mech. Dev. 61, 7–21.

Bertrand, V., Hudson, C., Caillol, D., Popovici, C., Lemaire, P., 2003. Neural tissue in ascidian embryos is induced by FGF9/16/20, acting via a combination of maternal GATA and Ets transcription factors. Cell 115, 615–627.

Bier, E., 2011. Evolution of development: diversified dorsoventral patterning. Curr. Biol., 21. http://dx.doi.org/10.1016/j.cub.2011.06.037.

Biffar, L., Stollewerk, A., 2015. Evolutionary variations in the expression of dorso-ventral patterning genes and the conservation of pioneer neurons in *Tribolium castaneum*. Dev. Biol. 400, 159–167. http://dx.doi.org/10.1016/j.ydbio.2015.01.025.

Biffar, L., Stollewerk, A., 2014. Conservation and evolutionary modifications of neuroblast expression patterns in insects. Dev. Biol. 388, 103–116. http://dx.doi.org/10.1016/j.ydbio.2014.01.028.

Blake, J.A., Grassle, J.P., Eckelbarger, K.J., 2009. *Capitella teleta*, a new species designation for the opportunistic and experimental *Capitella* sp. I, with a review of the literature for confirmed records. Zoosymposia 2, 25–53.

Boyer, B.C., Henry, J.J., Martindale, M.Q., 1998. The cell lineage of a polyclad turbellarian embryo reveals close similarity to coelomate spiralians. Dev. Biol. 204, 111–123. http://dx.doi.org/10.1006/dbio.1998.9084.

Boyer, B.C., Henry, J.Q., Martindale, M.Q., 1996. Dual origins of mesoderm in a basal spiralian: cell lineage analyses in the polyclad turbellarian *Hoploplana inquilina*. Dev. Biol. 179, 329–338. http://dx.doi.org/10.1006/dbio.1996.0264.

Boyle, M.J., Seaver, E.C., 2008. Developmental expression of foxA and gata genes during gut formation in the polychaete annelid, *Capitella* sp. I. Evol. Dev. 10, 89–105. http://dx.doi.org/10.1111/j.1525-142X.2007.00216.x.

Clement, A.C., 1962. Development of *Ilyanassa* following removal of the D macromere at successive cleavage stages. J. Exp. Zool. Part A 149, 193–215.

Clement, A.C., 1956. Experimental studies on germinal localization in *Ilyanassa*. J. Exp. Zool. Part A Ecol. Genet. Physiol. 132, 427–445.

Conklin, E.G., 1897. The embriology of *Crepidula*. J. Morphol. 13, 1–226.

Conzelmann, M., Offenburger, S., Asadulina, A., Keller, T., Münch, T.A., 2011.

Neuropeptides regulate swimming depth of *Platynereis* larvae. Proc. Natl. Acad. Sci. USA 108, E1174–E1183. http://dx.doi.org/10.1073/pnas.1109085108/-/DCSupplemental.www.pnas.org/cgi//10.1073/pnas.1109085108.
Costello, D.P., 1945. Experimental studies of germinal localization in *Nereis*. I. The development of isolated blastomeres. J. Exp. Zool. Part A 100, 19–66.
Davidson, E.H., 1990. How embryos work: a comparative view of diverse modes of cell fate specification. Development 108, 365–389.
Davis, G.K., D'Alessio, J.A., Patel, N.H., 2005. *Pax3/7* genes reveal conservation and divergence in the arthropod segmentation hierarchy. Dev. Biol. 285, 169–184. http://dx.doi.org/10.1016/j.ydbio.2005.06.014.
De Robertis, E.M., 2008. Evo-Devo: variations on ancestral themes. Cell 132, 185–195. http://dx.doi.org/10.1016/j.cell.2008.01.003.
De Robertis, E.M., Kuroda, H., 2004. Dorsal-Ventral patterning and neural induction in *Xenopus* embryos. Annu. Rev. Cell Dev. Biol. 20, 285–308. http://dx.doi.org/10.1146/annurev.cellbio.20.011403.154124.
De Robertis, E.M., Sasai, Y., 1996. A common plan for dorsoventral patterning in Bilateria. Nature 380, 37–40.
Demilly, A., Steinmetz, P., Gazave, E., Marchand, L., Vervoort, M., 2013. Involvement of the Wnt/β-catenin pathway in neurectoderm architecture in *Platynereis dumerilii*. Nat. Commun. 4, 1915. http://dx.doi.org/10.1038/ncomms2915.
Denes, A.S., Jékely, G., Steinmetz, P.R.H., Raible, F., Snyman, H., Prud'homme, B., Ferrier, D.E.K., Balavoine, G., Arendt, D., 2007. Molecular architecture of annelid nerve cord supports common origin of nervous system centralization in Bilateria. Cell 129, 277–288. http://dx.doi.org/10.1016/j.cell.2007.02.040.
Dickinson, A.J.G., Nason, J., Croll, R.P., 1999. Histochemical localization of FMRFamide, serotonin and catecholamines in embryonic *Crepidula fornicata* (Gastropoda, Prosobranchia). Zoomorphology 119, 49–62. http://dx.doi.org/10.1007/s004350050080.
Dictus, W.J., Damen, P., 1997. Cell-lineage and clonal-contribution map of the trochophore larva of *Patella vulgata* (Mollusca). Mech. Dev. 62, 213–226. http://dx.doi.org/10.1016/S0925-4773(97)00666-7.
Eisig, H.D., 1898. Zur Entwicklungsgeschichte der Capitelliden. Mitt. Zool. Stan. Neapel 13, 1–292.
Ferguson, E.L., Anderson, K.V., 1992. Localized enhancement and repression of the activity of the TGF-beta family member, Decapentaplegic, is necessary for dorsal-ventral pattern formation in the *Drosophila* embryo. Development 114, 583–597.
Goldstein, B., 1993. Establishment of gut fate in the E lineage of *C. elegans*: the roles of lineage-dependent mechanisms and cell interactions. Development 118, 1267–1277.
Gómez-Skarmeta, J.L., Campuzano, S., Modolell, J., 2003. Half a century of neural prepatterning: the story of a few bristles and many genes. Nat. Rev. Neurosci. 4, 587–598. http://dx.doi.org/10.1038/nrn1142.
Grassle, J.P., Grassle, J.F., 1976. Sibling species in the marine pollution indicator *Capitella* (Polychaeta). Science 192, 567–569.
Hashimoto, N., Kurita, Y., Wada, H., 2012. Developmental role of dpp in the gastropod shell plate and co-option of the dpp signaling pathway in the evolution of the operculum. Dev. Biol. 366, 367–373. http://dx.doi.org/10.1016/j.ydbio.2012.04.010.
Hejnol, A., 2010. A twist in time–the evolution of spiral cleavage in the light of animal phylogeny. Integr. Comp. Biol. 50, 695–706. http://dx.doi.org/10.1093/icb/icq103.
Hejnol, A., Lowe, C.J., 2015. Embracing the comparative approach: how robust phylogenies and broader developmental sampling impacts the understanding of nervous system evolution. Philos. Trans. R. Soc. Lond. B. Biol. Sci. 370, 20150045.
Hejnol, A., Martindale, M.Q., Henry, J.Q., 2007. High-resolution fate map of the snail *Crepidula fornicata*: the origins of ciliary bands, nervous system, and muscular elements. Dev. Biol. 305, 63–76. http://dx.doi.org/10.1016/j.ydbio.2007.01.044.
Henry, J.J., 1986. The role of unequal cleavage and the polar lobe in the segregation of developmental potential during first cleavage in the embryo of *Chaetopterus variopedatus*. Roux's Arch. Dev. Biol. 195, 103–116. http://dx.doi.org/10.1007/BF00456106.
Henry, J.J., Perry, K.J., 2008. MAPK activation and the specification of the D quadrant in the gastropod mollusc, *Crepidula fornicata*. Dev. Biol. 313, 181–195. http://dx.doi.org/10.1016/j.ydbio.2007.10.019.
Henry, J.J., Perry, K.J., Fukui, L., Alvi, N., 2010. Differential localization of mRNAs during early development in the mollusc, *Crepidula fornicata*. Integr. Comp. Biol. 50, 720–733. http://dx.doi.org/10.1093/icb/icq088.
Henry, J.Q., 2014. Spiralian model systems. Int. J. Dev. Biol. 58, 389–401. http://dx.doi.org/10.1387/ijdb.140127jh.
Henry, J.Q., Hejnol, A., Perry, K.J., Martindale, M.Q., 2007. Homology of ciliary bands in spiralian trochophores. Integr. Comp. Biol. 47, 865–871. http://dx.doi.org/10.1093/icb/icm035.
Henry, J.Q., Martindale, M.Q., 1998. Conservation of the spiralian developmental program: cell lineage of the nemertean, *Cerebratulus lacteus*. Dev. Biol. 201, 253–269. http://dx.doi.org/10.1006/dbio.1998.8966.
Henry, J.Q., Okusu, A., Martindale, M.Q., 2004. The cell lineage of the polyplacophoran, *Chaetopleura apiculata*: variation in the spiralian program and implications for molluscan evolution. Dev. Biol. 272, 145–160. http://dx.doi.org/10.1016/j.ydbio.2004.04.027.
Henry, J.Q., Perry, K.J., Martindale, M.Q., 2006. Cell specification and the role of the polar lobe in the gastropod mollusc *Crepidula fornicata*. Dev. Biol. 297, 295–307. http://dx.doi.org/10.1016/j.ydbio.2006.04.441.
Herpin, A., Lelong, C., Becker, T., Favrel, P., Cunningham, C., 2007. A tolloid homologue from the Pacific oyster *Crassostrea gigas*. Gene Expr. Patterns 7, 700–708. http://dx.doi.org/10.1016/j.modgep.2007.03.001.
Hill, S.D., Boyer, B.C., 2001. Phalloidin labeling of developing muscle in embryos of the polychaete *Capitella* sp. I.. Biol. Bull. 201, 257–258.
Huang, F.Z., Kang, D., Ramirez-Weber, F.A., Bissen, S.T., Weisblat, D.A., 2002. Micromere lineages in the glossiphoniid leech *Helobdella*. Development 129, 719–732.
Hudson, C., 2003. A conserved role for the MEK signalling pathway in neural tissue specification and posteriorisation in the invertebrate chordate, the ascidian *Ciona intestinalis*. Development 130, 147–159. http://dx.doi.org/10.1242/dev.00200.
Iijima, M., Takeuchi, T., Sarashina, I., Endo, K., 2008. Expression patterns of *engrailed* and *dpp* in the gastropod *Lymnaea stagnalis*. Dev. Genes Evol. 218, 237–251. http://dx.doi.org/10.1007/s00427-008-0217-0.
Irish, V.F., Gelbart, W.M., 1987. The *decapentaplegic* gene is required for dorsal-ventral patterning of the *Drosophila* embryo. Genes Dev. 1, 868–879. http://dx.doi.org/10.1101/gad.1.8.868.
Jägersten, G., 1972. Evolution of the Metazoan Life Cycle. A Comprehensive Theory. Acad. Press, 282.
Jékely, G., Colombelli, J., Hausen, H., Guy, K., Stelzer, E., Nédélec, F., Arendt, D., 2008. Mechanism of phototaxis in marine zooplankton. Nature 456, 395–399. http://dx.doi.org/10.1038/nature07590.
Kin, K., Kakoi, S., Wada, H., 2009. A novel role for dpp in the shaping of bivalve shells revealed in a conserved molluscan developmental program. Dev. Biol. 329, 152–166. http://dx.doi.org/10.1016/j.ydbio.2009.01.021.
Kingsley, E.P., Chan, X.Y., Duan, Y., Lambert, J.D., 2007. Widespread RNA segregation in a spiralian embryo. Evol. Dev. 9, 529–539.
Kozin, V.V., Babakhanova, R.A., Kostyuchenko, R.P., 2013. Functional role for MAP kinase signaling in cell lineage and dorsoventral axis specification in the basal gastropod *Testudinalia testudinalis* (Patellogastropoda, Mollusca). Russ. J. Dev. Biol. 44, 35–47. http://dx.doi.org/10.1134/S1062360413010025.
Kumano, G., Nishida, H., 2007. Ascidian embryonic development: an emerging model system for the study of cell fate specification in chordates. Dev. Dyn.. http://dx.doi.org/10.1002/dvdy.21108.
Kuo, D.-H., Weisblat, D.A., 2011. A new molecular logic for BMP-mediated dorsoventral patterning in the leech *Helobdella*. Curr. Biol. 21, 1282–1288. http://dx.doi.org/10.1016/j.cub.2011.06.024.
Lambert, J.D., 2010. Developmental patterns in spiralian embryos. Curr. Biol. 20, R72–7. http://dx.doi.org/10.1016/j.cub.2009.11.041.
Lambert, J.D., 2008. Mesoderm in spiralians: the organizer and the 4d cell. J. Exp. Zool. B: Mol. Dev. Evol. 310B, 15–23. http://dx.doi.org/10.1002/jez.b.
Lambert, J.D., Johnson, A.B., Hudson, C.N., Chan, A., 2016. Dpp/BMP2-4 mediates signaling from the D-Quadrant organizer in a spiralian embryo. Curr. Biol. 26, 2003–2010. http://dx.doi.org/10.1016/j.cub.2016.05.059.
Lambert, J.D., Nagy, L.M., 2002. Asymmetric inheritance of centrosomally localized mRNAs during embryonic cleavages. Nature 420, 682–686. http://dx.doi.org/10.1038/nature01188.1.
Lambert, J.D., Nagy, L.M., 2001. MAPK signaling by the D quadrant embryonic organizer of the mollusc *Ilyanassa obsoleta*. Development 56, 45–56.
Lea, R., Papalopulu, N., Amaya, E., Dorey, K., 2009. Temporal and spatial expression of FGF ligands and receptors during *Xenopus* development. Dev. Dyn. 238, 1467–1479. http://dx.doi.org/10.1002/dvdy.21913.
Lowe, C.J., Terasaki, M., Wu, M., Freeman, R.M., Runft, L., Kwan, K., Haigo, S., Aronowicz, J., Lander, E., Gruber, C., Smith, M., Kirschner, M., Gerhart, J., 2006. Dorsoventral patterning in hemichordates: insights into early chordate evolution. PLoS Biol. 4, 1603–1619. http://dx.doi.org/10.1371/journal.pbio.0040291.
Lynch, J.A., Roth, S., 2011. The evolution of dorsal-ventral patterning mechanisms in insects. Genes Dev.. http://dx.doi.org/10.1101/gad.2010711.
Marlow, H., Tosches, M.A., Tomer, R., Steinmetz, P.R., Lauri, A., Larsson, T., Arendt, D., 2014. Larval body patterning and apical organs are conserved in animal evolution. BMC Biol. 12, 7. http://dx.doi.org/10.1186/1741-7007-12-7.
Martindale, M.Q., Doe, C.Q., Morrill, J.B., 1985. The role of animal-vegetal interaction with respect to the determination of dorsoventral polarity in the equal-cleaving spiralian, *Lymnaea palustris*. Roux's Arch. Dev. Biol. 194, 281–295.
Mead, A.D., 1897. The early development of marine annelids. J. Morphol. 13, 227–327.
Meyer, N.P., Boyle, M.J., Martindale, M.Q., Seaver, E.C., 2010. A comprehensive fate map by intracellular injection of identified blastomeres in the marine polychaete *Capitella teleta*. Evodevo 1, 8. http://dx.doi.org/10.1186/2041-9139-1-8.
Meyer, N.P., Carrillo-Baltodano, A., Moore, R.E., Seaver, E.C., 2015. Nervous system development in lecithotrophic larval and juvenile stages of the annelid *Capitella teleta*. Front. Zool. 12, 15. http://dx.doi.org/10.1186/s12983-015-0108-y.
Meyer, N.P., Seaver, E.C., 2010. Cell lineage and fate map of the primary somatoblast of the polychaete annelid *Capitella teleta*. Integr. Comp. Biol. 50, 756–767. http://dx.doi.org/10.1093/icb/icq120.
Meyer, N.P., Seaver, E.C., 2009. Neurogenesis in an annelid: characterization of brain neural precursors in the polychaete *Capitella* sp. I. Dev. Biol. 335, 237–252. http://dx.doi.org/10.1016/j.ydbio.2009.06.017.
Minokawa, T., Yagi, K., Makabe, K.W., Nishida, H., 2001. Binary specification of nerve cord and notochord cell fates in ascidian embryos. Development 128, 2007–2017.
Muñoz-Sanjuán, I., Brivanlou, A.H., 2002. Neural induction, the default model and embryonic stem cells. Nat. Rev. Neurosci. 3, 271–280. http://dx.doi.org/10.1038/nrn786.
Nakamoto, A., Nagy, L.M., Shimizu, T., 2010. Secondary embryonic axis formation by transplantation of D quadrant micromeres in an oligochaete annelid. Development 138, 283–290. http://dx.doi.org/10.1242/dev.055384.
Nakamura, T., Shiomi, I., Shimizu, T., 2017. Embryonic expression of *festina lente* (*fel*), a novel maternal gene, in the oligochaete annelid *Tubifex tubifex*. Gene Expr. Patterns 25–26, 29–35. http://dx.doi.org/10.1016/j.gep.2017.05.001.
Nederbragt, A.J., van Loon, A.E., Dictus, W.J., 2002. Expression of *Patella vulgata* orthologs of *engrailed* and *dpp-BMP2/4* in adjacent domains during molluscan shell development suggests a conserved compartment boundary mechanism. Dev. Biol. 246, 341–355. http://dx.doi.org/10.1006/dbio.2002.0653.

Nielsen, C., 2012. How to make a protostome. Invertebr. Syst. 26, 25–40. http://dx.doi.org/10.1071/IS11041.
Nielsen, C., 2005. Trochophora larvae and adult body regions in annelids: some conclusions. Hydrobiologia 535–536, 23–24. http://dx.doi.org/10.1007/s10750-004-1404-2.
Nielsen, C., 2004. Trochophora larvae: cell-lineages, ciliary bands, and body regions. 1. Annelida and Mollusca. J. Exp. Zool. B: Mol. Dev. Evol. 302, 35–68. http://dx.doi.org/10.1002/jez.b.20001.
Novikoff, A.B., 1938. Embryonic determination in the annelid *Sabella vulgaris*. II. Transplantation of polar lobes and blastomeres as a test of their inducing capacities. Biol. Bull. 74, 211–234.
Pera, E.M., Ikeda, A., Eivers, E., De Robertis, E.M., 2003. Integration of IGF, FGF, and anti-BMP signals via Smad1 phosphorylation in neural induction. Genes Dev. 17, 3023–3028. http://dx.doi.org/10.1101/gad.1153603.
Rabinowitz, J.S., Lambert, J.D., 2010. Spiralian quartet developmental potential is regulated by specific localization elements that mediate asymmetric RNA segregation. Development 137, 4039–4049. http://dx.doi.org/10.1242/dev.055269.
Randel, N., Asadulina, A., Bezares-Calderón, L.A., Verasztó, C., Williams, E.A., Conzelmann, M., Shahidi, R., Jékely, G., 2014. Neuronal connectome of a sensory-motor circuit for visual navigation. Elife 3, 1–22. http://dx.doi.org/10.7554/eLife.02730.
Render, J., 1997. Cell fate maps in the *Ilyanassa obsoleta* embryo beyond the third division. Dev. Biol. 189, 301–310. http://dx.doi.org/10.1006/dbio.1997.8654.
Render, J., 1991. Fate maps of the first quartet micromeres in the gastropod *Ilyanassa obsoleta*. Development 501, 495–501.
Rentzsch, F., Bakkers, J., Kramer, C., Hammerschmidt, M., 2004. Fgf signaling induces posterior neuroectoderm independently of Bmp signaling inhibition. Dev. Dyn. 231, 750–757. http://dx.doi.org/10.1002/dvdy.20244.
Reverberi, G., 1971. Annelids, Experimental Embryology of Marine and Fresh-water Invertebrates. North-Holland Publishing Company, Amsterdam.
Rhode, B., 1993. Larval and adult eyes in *Capitella* spec. I (Annelida, Polychaeta). J. Morphol. 217, 327–335. http://dx.doi.org/10.1002/jmor.1052170307.
Seaver, E.C., Thamm, K., Hill, S.D., 2005. Growth patterns during segmentation in the two polychaete annelids, *Capitella* sp. I and *Hydroides elegans*: comparisons at distinct life history stages. Evol. Dev. 7, 312–326. http://dx.doi.org/10.1111/j.1525-142X.2005.05037.x.
Shankland, M., 1995. Formation and specification of neurons during the development of the leech central nervous system. J. Neurobiol. 27, 294–309. http://dx.doi.org/10.1002/neu.480270304.
Skeath, J.B., 1998. The *Drosophila* EGF receptor controls the formation and specification of neuroblasts along the dorsal-ventral axis of the *Drosophila* embryo. Development 125, 3301–3312.
Stern, C.D., 2006. Neural induction: 10 years on since the “default model”. Curr. Opin. Cell Biol. 18, 692–697. http://dx.doi.org/10.1016/j.ceb.2006.09.002.
Stern, C.D., 2005. Neural induction: old problem, new findings, yet more questions. Development 132, 2007–2021. http://dx.doi.org/10.1242/dev.01794.
Strathmann, M.F., 1987. Reproduction and Development of Marine Invertebrates of the Northern Pacific Coast. Data and Methods for the Study of Eggs, Embryos, and Larvae. University of Washington Press, 682.
Suryamohan, K., Hanson, C., Andrews, E., Sinha, S., Scheel, M.D., Halfon, M.S., 2016. Redeployment of a conserved gene regulatory network during *Aedes aegypti* development. Dev. Biol. 416, 402–413. http://dx.doi.org/10.1016/j.ydbio.2016.06.031.
Sweet, H.C., 1998. Specification of first quartet micromeres in *Ilyanassa* involves inherited factors and position with respect to the inducing D macromere. Development 125, 4033–4044.
Tan, S., Huan, P., Liu, B., 2017. Expression patterns indicate that BMP2/4 and Chordin, not BMP5-8 and Gremlin, mediate dorsal-ventral patterning in the mollusk *Crassostrea gigas*. Dev. Genes Evol. 227, 75–84. http://dx.doi.org/10.1007/s00427-016-0570-3.
Thorpe, C.J., Schlesinger, A., Carter, J.C., Bowerman, B., 1997. Wnt signaling polarizes an early *C. elegans* blastomere to distinguish endoderm from mesoderm. Cell 90, 695–705.
Torrence, S.A., Law, M.I., Stuart, D.K., 1989. Leech neurogenesis. II. Mesodermal control of neuronal patterns. Dev. Biol. 136, 40–60. http://dx.doi.org/10.1016/0012-1606(89)90129-2.
Tosches, M.A., Bucher, D., Vopalensky, P., Arendt, D., 2014. Melatonin signaling controls circadian swimming behavior in marine zooplankton. Cell 159, 46–57. http://dx.doi.org/10.1016/j.cell.2014.07.042.
True, J.R., Haag, E.S., 2001. Developmental system drift and flexibility in evolutionary trajectories. Evol. Dev. 3, 109–119. http://dx.doi.org/10.1046/j.1525-142X.2001.003002109.x.
von Ohlen, T., Doe, C.Q., 2000. Convergence of dorsal, dpp, and egfr signaling pathways subdivides the *Drosophila* neuroectoderm into three dorsal-ventral columns. Dev. Biol. 224, 362–372. http://dx.doi.org/10.1006/dbio.2000.9789.
Wanninger, A., 2008. Comparative lophotrochozoan neurogenesis and larval neuroanatomy: recent advances from previously neglected taxa. Acta Biol. Hung. 59 (Suppl.), 127–136. http://dx.doi.org/10.1556/ABiol.59.2008.Suppl.21.
Weisblat, D.A., Kim, S.Y., Stent, G.S., 1984. Embryonic origins of cells in the leech *Helobdella triserialis*. Dev. Biol. 104, 65–85. http://dx.doi.org/10.1016/0012-1606(84)90037-X.
Wikramanayake, A.H., Klein, W.H., 1997. Multiple signaling events specify ectoderm and pattern the oral-aboral axis in the sea urchin embryo. Development 20, 13–20.
Williams, E.A., Conzelmann, M., Jékely, G., 2014. Myoinhibitory peptide regulates feeding in the marine annelid *Platynereis*. Front. Zool. 12, 1.
Williams, E.A., Verasztó, C., Jasek, S., Conzelmann, M., Shahidi, R., Bauknecht, P., Jékely, G., 2017. Synaptic and peptidergic connectome of a neurosecretory centre in the annelid brain. bioRxiv. doi: ⟨http://dx.doi.org/10.1101/115204⟩.
Wilson, E.B., 1904a. Experimental studies on germinal localization. I. The germ-regions in the egg of *Dentalium*. J. Exp. Zool. Part A 1, 1–72.
Wilson, E.B., 1904b. Experimental studies in germinal localization. II. Experiments on the cleavage-mosaic in *Patella* and *Dentalium*. Development 1, 197–268.
Wilson, E.B., 1892. The cell lineage of *Nereis*: a contribution to the cytogeny of the annelid body. J. Morphol. 6, 361–480.
Wilson, M.J., Kenny, N.J., Dearden, P.K., 2014. Components of the dorsal-ventral pathway also contribute to anterior-posterior patterning in honeybee embryos (*Apis mellifera*). Evodevo 5, 11. http://dx.doi.org/10.1186/2041-9139-5-11.
Wilson, S.I., Edlund, T., 2001. Neural induction: toward a unifying mechanism. Nat. Neurosci. 4, 1161–1168. http://dx.doi.org/10.1038/nn747.
Xu, F., Domazet-Lošo, T., Fan, D., Dunwell, T.L., Li, L., Fang, X., Zhang, G., 2016. High expression of new genes in trochophore enlightening the ontogeny and evolution of trochozoans. Sci. Rep. 6, 34664. http://dx.doi.org/10.1038/srep34664.
Yamaguchi, E., Dannenberg, L.C., Amiel, A.R., Seaver, E.C., 2016. Regulative capacity for eye formation by first quartet micromeres of the polychaete *Capitella teleta*. Dev. Biol. 410, 119–130. http://dx.doi.org/10.1016/j.ydbio.2015.12.009.
Yamaguchi, E., Seaver, E.C., 2013. The importance of larval eyes in the polychaete *Capitella teleta*: effects of larval eye deletion on formation of the adult eye. Invertebr. Biol. 132, 352–367. http://dx.doi.org/10.1111/ivb.12034.
Zantke, J., Ishikawa-Fujiwara, T., Arboleda, E., Lohs, C., Schipany, K., Hallay, N., Straw, A.D., Todo, T., Tessmar-Raible, K., 2013. Circadian and circalunar clock interactions in a marine annelid. Cell Rep. 5, 99–113. http://dx.doi.org/10.1016/j.celrep.2013.08.031.